ISEF 2005 - XII International Symposium on Electromagnetic Fields
in Mechatronics, Electrical and Electronic Engineering
Baiona, Spain, September 15-17, 2005

COMPARISON OF 2D FEM SIMULATION AND ANALYTICAL CALCULATION OF THE SHORT-CIRCUIT BEHAVIOUR OF A PERMANENT-MAGNET SYNCHRONOUS MACHINE

M. Herranz Gracia, K. Hameyer

Institute of Electrical Machines, RWTH Aachen University
Schinkelstraße 4, D-52062 Aachen, Germany
Mercedes.HerranzGracia@iem.rwth-aachen.de

Abstract **– *The use of Permanent-Magnet Synchronous Machine (PMSM) as servo drive has increased in recent years. Therefore, the PMSM's behaviour in short-circuit operation is of high interest. Here, the simulation of both, analytical and numerical model is conducted. The results are compared and discussed.***

I. Introduction

Since the introduction of high-energy permanent-magnet materials, the PMSM has become a competitive choice in variable speed applications. The classical use of synchronous machines in power generation explains the fact that most short-circuit studies of it are performed at network frequency [1]. However, using the PMSM in a servo application, the variation of the short-circuit torque and current with the speed and the possible de-magnetisation of the permanent magnets are a crucial issue. Here, a 2D FE model with a circuit coupling is applied to compute the interesting electrical quantities. In addition, an analytical model is generated with the data from the quasi static FE model to compare its short-circuit results with those obtained from the transient FE model. The FE Model is simulated by iMOOSE [2].

II. FE Model

The studied machine is a large permanent-magnet synchronous-machine with 3-phases, 16 poles and two parallel branches per phase. The regions of the FE model corresponding to stator coils are defined as stranded conductors connected to the external electrical circuit as shown in Fig. 1.

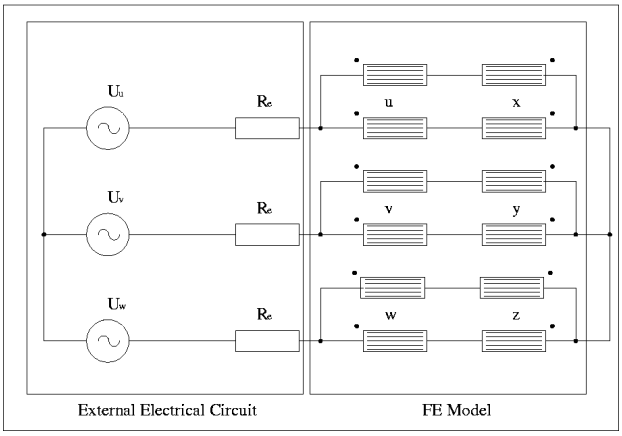

Fig. 1: Connection of the FE Model and the external circuit.

The voltage drop across the stranded conductor k is calculated from [3]:

$$\Delta V_k = R_k' \cdot I_k + \frac{l \cdot w}{F_k} \int_{F_k} \frac{\mathrm{d}}{\mathrm{d}t} A \cdot \mathrm{d}F_k \tag{1}$$

$$R_k' = \frac{l \cdot w}{\lambda \cdot F_k^2} \int_{F_k} \frac{1}{\sigma} \mathrm{d}F_k, \tag{2}$$

where l is the length of the machine, w the number of turns of the coil, λ the coil fill factor, A the magnetic vector potential and F_k the total area of the conductor. The resistance R_k' and the integral term of the voltage drop expression represent the winding's copper resistance and its inductance. Therefore, both are not inserted in the circuit explicitly. The extra resistances R_e shown in Fig. 1 represents the windings overhang resistance. It is calculated as the measured resistance per phase of the machine minus the resistance of the copper conductors R_k' in the FE model.

III. Analytical Model

The analytical model of the machine consists of the differential equations of the machine: voltage equations (Eq. 3 and 4), flux linkage equations (Eq. 5 and 6) and torque equation (Eq. 7) in the rotor d-q frame [4]:

$$u_{1d} = i_{1d} R_1 + \frac{d\psi_{1d}}{dt} - p\omega\psi_{1q} \tag{3}$$

$$u_{1q} = i_{1q} R_1 + \frac{d\psi_{1q}}{dt} - p\omega\psi_{1d} \tag{4}$$

$$\psi_{1d} = i_{1d} L_{1d} + \psi_{1f} \tag{5}$$

$$\psi_{1q} = i_{1q} L_{1q} \tag{6}$$

$$m_i = \frac{3}{2} p(\psi_{1d} i_{1q} - \psi_{1q} i_{1d}) \tag{7}$$

The speed of the machine is assumed to be constant during short-circuit operation. Therefore, the motion equation is not included in the model. The d-axis inductance L_{1d}, the q-axis inductance L_{1q}, the rotor flux linkage ψ_{1f} , and the resistance per phase R_1 are used as parameter. They are derived from the FE model with the exception of the resistance, which is measured.

Ψ_{1f} is calculated from the computation of the machine at no-load operation. Then the flux linkage through the windings corresponds to the rotor flux linkage. It is calculated by:

$$\psi_{1f} = \phi_{1f} \cdot w = \left(\frac{\int_{S_{u=}} \vec{A}_z \cdot d\vec{S}_{u+}}{\int_{S_{u+}} d\vec{S}_{u+}'} - \frac{\int_{S_{u-}} \vec{A}_z \cdot d\vec{S}_{u-}}{\int_{S_{u-}} d\vec{S}_{u-}} \right) \cdot l \cdot w \tag{8}$$

where S_{u+} are the conductor regions with $+I_u$ and S_{u-} these with $-I_u$. The variation of ψ_{1f} with the rotor position (electrical angle) for two different magnet temperatures (20 and 150° C) is plotted in Fig. 2

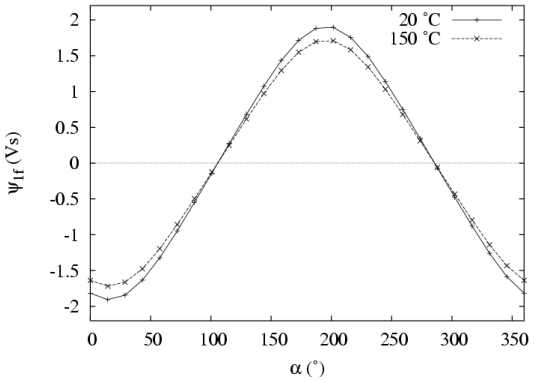

Fig. 2: Rotor flux linkage.

L_{1d} and L_{1q} are derived from the FE model simulation with the nominal current I_n and without remanence in the magnets. The phase of the current ε is defined so that for $\varepsilon=0$ the current is in the rotor-defined negative d-axis and for $\varepsilon=90°$ it is in the q-axis. The synchronous inductance L_{1s} of the machine is calculated by:

$$L_{1s} = \frac{\psi}{I}. \tag{9}$$

The flux linkage is computed with Eq. (8). L_{1s} depending on ε is plotted in Fig. 3. By definition L_{1d} is the synchronous inductance for $\varepsilon=0$ and L_{1q} for $\varepsilon=90°$.

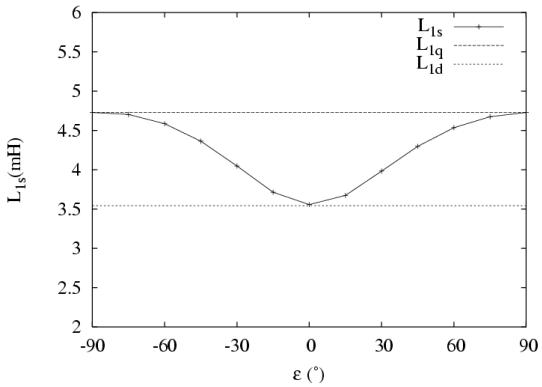

Fig. 3: Synchronous inductance.

IV. Results

A three-phase short-circuit is simulated both with the analytical and the FE model. The machine is operated at nominal speed. Symmetrical voltages are applied to the machine in the first part of the study. Then they are simultaneously set to zero for the three phases. The stator winding is short-circuited at zero voltage in one of the phases (see Fig. 4). In this case, the highest current peak occurs.

In Fig. 5, the results for torque and current are plotted. It is remarkable that the current in phase v only reaches a value of twice the nominal current, although it is the worst case scenario. This is due to the following two reasons:

- In absence of excitation and damper winding the sub-transient-reactance in the d-axis X_d'' is equal to the d-static reactance X_d. The higher current is inversely proportional to X_d''. In a machine with electrical excitation X_d'' is much smaller than X_d, which result in much higher current peaks.

- The time constant of the stator is of the same order as the electric period of the machine. The stationary state is reached after about three periods and therefore the attenuation of the transitory is fast.

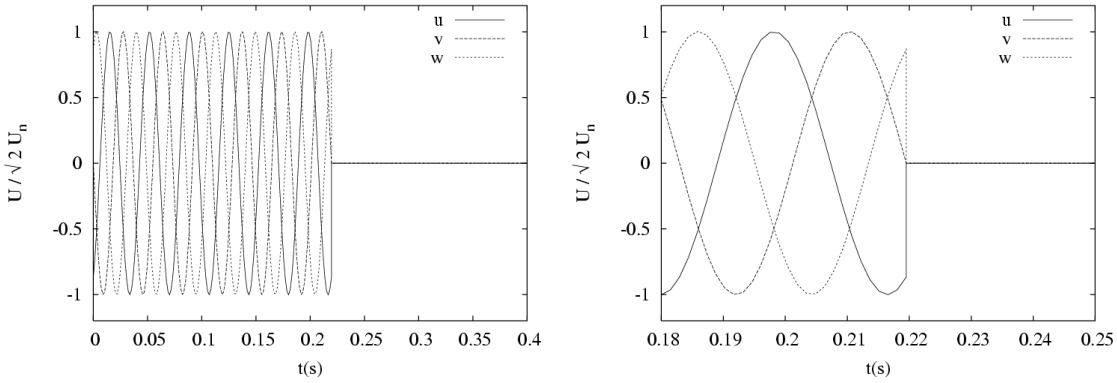

Fig. 4: Voltage applied to the machine.

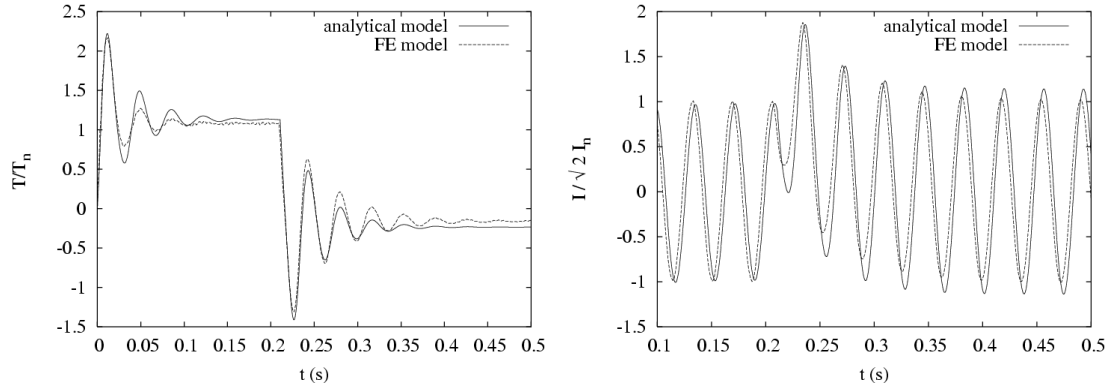

(a) (b)

Fig. 5: (a) Torque from the nominal point to the short-circuit operation.
(b) Current of the phase v from the nominal point to the short-circuit operation.

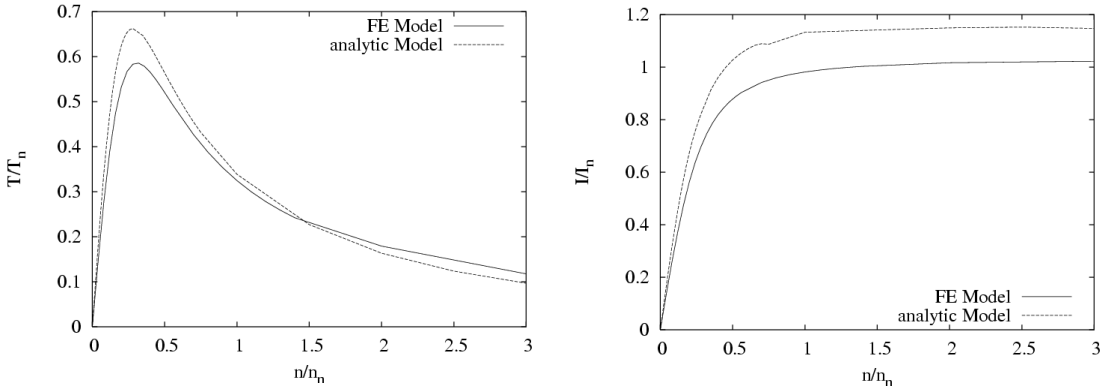

(a) (b)

Fig. 6: (a) Static short-circuit torque at different speeds.
(b) Sustained short-circuit current at different speeds.

The same study is performed at different speeds of the machine. The static short-circuit torque and the sustained short-circuit current are shown in Fig. 6.

The static short-circuit torque shows a theoretical maximum according to [5] at:

$$\upsilon = \frac{n}{n_0} = \frac{R}{X_{d0}} = \frac{R}{2\pi \cdot p \cdot n_0 \cdot L_d} = 0.281 \tag{7}$$

and tends to zero both, when the speed is zero and infinite. The sustained short-circuit current is zero at zero speed and increases with the speed to reach an almost constant value at about the nominal speed.

The comparison of the results of both models is shown in Table 1. The measured values are not yet available.

	FE model	Analytical model	Difference
υ	0.298	0.280	6 %
$\frac{M_{\max}}{M_n}$	0.584	0.661	12%
$\frac{I_k}{I_n}$	1.029	1.147	10%

Table 1: Comparison of the results of both models.

The results from both models differ. The use of the analytical model brings both a larger static short-circuit torque and sustained short-circuit current. That is due to two reasons:

- The saturation conditions in the short-circuit case are not the same as at nominal load. In general a different level of saturation is reached at short-circuit operation when compared to no-load.
- The PM operation point changes from the nominal load to the short-circuit case. Fig. 7 plots the evolution of the rotor flux from the nominal to the short-circuit operation. It is substantially higher for nominal operation than for short-circuit operation.

For the analytical model the inductances and the rotor flux linkage are derived respectively from the nominal working point and the no load point.

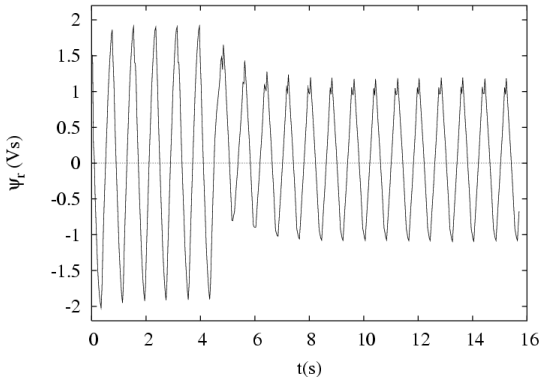

Fig. 7: Rotor flux linkage from nominal to short-circuit operation.

In a next step the de-magnetisation of the PM is studied. The minimal flux-density in the magnets is compared for nominal operation I_n, maximal short-circuit current I_s and sustained short-circuit current I_k. The results are shown in Fig. 8. The sections between α=0 and 2.5°, 20 and 25°, etc. do not correspond to PM-material but to steel yokes in the pole gap between the magnets. The flux-density and the magnetic field strength values in the magnets are far from the non-recoverable de-magnetisation (H_c=-900 *kA/m*, B=-0.35 *T*) as it can be seen in Table 2.

	I_n	I_s	I_k	Non-recoverable de-magnetisation
B_{min} (T)	0.48	0.17	0.42	-0.35
H_{min} (kA/m)	347	123	304	-900

Table 2: Comparison of the minimal flux density and the minimal magnetic field strength of the magnets with the non-recoverable de-magnetisation values.

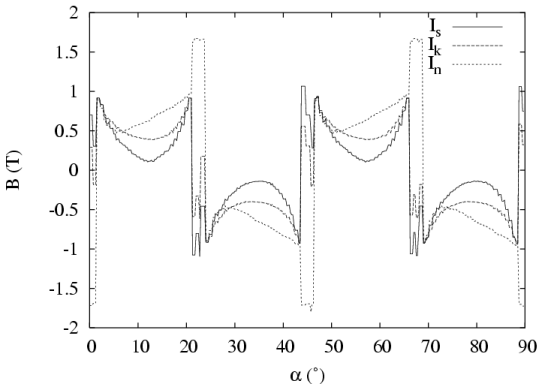

Fig. 8: Flux density in the PM's.

V. Conclusion

Two models are used to study the short-circuit behaviour of a PMSM. The FE model is coupled to an external circuit, which defines the connection of the stator windings. The FE model is also used to determine the parameters, which are used in the analytical model. The latter consists of the differential equations of the machine in the rotor d-q frame.

The results of the short-circuit simulation of a PMSM are presented. They are calculated both, numerically (FE) and analytically. The analytical approach applied here is much faster but cannot cope well with the saturation effects, the change in the operating point of the magnets and their possible de-magnetisation. The differences are up to 12% for the torque, what means that these factors are not negligible. According to that, further investigations should be done to find an analytical formulation, which can consider these aspects for first try computations avoiding high costs of using FEM.

References

[1] R. Wamkeue and I. Kamwa, "Line-to-line short-circuit-based finite-element performance and parameter predictions of large hydro generators", *IEEE Transactions on Energy Conversion*, vol. 18, pp. 370-378, September 2003.

[2] http://iMOOSE.sourceforge.net, Innovative Modern Object-Oriented Solver Environment, Institute of Electrical Machines, RWTH Aachen University

[3] G. Arians and G. Henneberger, "Object oriented analysis and design of transient finite element solvers applied to coupled problems", in *9th Conference on Electromagnetic Field Computation*, (Milwaukee, USA), CEFC, 2000.

[4] P. Vas, "Vector Control of AC Machines", Oxford Science Publications, 1990.

[5] G. Müller, "Grundlagen elektrische Maschinen ", VCH Verlaggesellschaft, 1994.